Pertanika J. Sci. & Technol. 30 (2): 1717 - 1738 (2022)

PERTANIKA JOURNALS

SCIENCE & TECHNOLOGY

Journal homepage: http://www.pertanika.upm.edu.my/

Gaussian and Mean Curvature of Biquintic Trigonometric Bézier Surface

Anis Solehah Mohd Kamarudzaman, Nurul Huda Mohamad Nasir and Md Yushalify Misro*

School of Mathematical Sciences, Universiti Sains Malaysia, 11800 USM, Gelugor, Pulau Pinang, Malaysia

ABSTRACT

Bézier curves and surfaces are very important in many areas, especially the manufacturing and aerospace. Surface inspection through visualisation is required to create high-quality surfaces and reduce unwanted products. The smoothness of the surface can be quantified using curvature. In this research, different surfaces types will be generated using the quintic trigonometric Bézier basis function. All the surfaces will be evaluated and analysed using Gaussian and mean curvature. Finally, curvature for each surface type will be mapped using colour-coded mapping and can be further characterised based on their positive and negative curvature values. This insight can also help the designer produce a smooth surface and develop quality products.

Keywords: Biquintic trigonometric Bézier surface, curvature analysis, Gaussian curvature, mean curvature

INTRODUCTION

Bézier curve is one of the many manifestations in Computer Aided Geometric Design (CAGD). Numerous studies of the Bézier curve involving the new creation of the basis function have been come to light and captured much attention from plentiful of researchers. Diverse creation of the new basis function from A-class of Bézier-like (Chen & Wang, 2003) to trigonometric Bézier (Tan & Zhu, 2019, Ammad et al., 2022) to hybrid Bézier (Bibi et al., 2021), and the recent one is fractional Bézier curve (Zain et al., 2021).

ARTICLE INFO

Article history:
Received: 25 October 2021
Accepted: 28 December 2021
Published: 31 March 2022

DOI: https://doi.org/10.47836/pjst.30.2.46

E-mail addresses:
anysleha@gmail.com (Anis Solehah Mohd Kamarudzaman)
hudanasir236@gmail.com (Nurul Huda Mohamad Nasir)
yushalify@usm.my (Md Yushalify Misro)
*Corresponding author

ISSN: 0128-7680
e-ISSN: 2231-8526

For example, the idea of the quintic trigonometric Bézier curve (Misro et al., 2017) has been applied to several applications, including curve fitting (Adnan et al., 2020), continuous surface construction (Ismail & Misro, 2020), and analysis of the adjustable parameter (Misro et al., 2019). The authors also included the importance of the curvature in determining a fair curve.

According to Bartkowiak and Brown (2019), the curvature is an indicative measure of the smoothness of the topological surface. Thus, the curvature is one of the essential measures to interpret the geometry appearance of curves and surfaces in geometric modelling. For surface modelling, Gaussian and mean curvature can be derived from fundamental concepts in differential geometry, as discussed in Pressley (2010) and Farin (2014).

In 2003, Zheng and Sederberg derived Gaussian and mean curvature formulas for rational Bézier tensor-product and triangular patch. Different computational approaches for local estimation of Gaussian and mean curvature are discussed with analytical values of geometric objects are compared in Magid et al. (2007). Meanwhile, a new method called local surface fitting for estimating surface curvature has been described by Razdan and Bae (2005).

Curvature analysis or surface interrogation gives an understanding of how the surface behaves. A few methods can illustrate the curvature on the surface for the curvature analysis, including colour mapping, as explained in Hahmann (1999). Moreover, Dill (1981) and Beck et al. (1986) discussed the colour mapping technique for surface curvature analysis. Indeed, both authors agreed that the colour mapping approach is convenient for illustrating the surface curvature.

The shape of surfaces plays a vital role in the manufacturing industry and geometric modelling. However, there are some possibilities in the manufacturing industry that residual stresses can cause deformation thus produce damaged products (Garcia et al., 2021). Apart from the manufacturing industry, the aerospace industry will also be affected by this problem, creating significant loss deprivation. Thus, checking the quality of the product's surface design is very crucial.

Due to the lack of research in surface curvature analysis, this paper will focus on determining Gaussian and mean curvatures on different types of biquintic trigonometric Bézier surfaces. This research will also visualise the surface curvature using colour mapping and classify each Gaussian and mean curvature of different biquintic trigonometric Bézier surfaces based on positive and negative curvature values.

METHODOLOGY

This section explains the properties of the quintic trigonometric Bézier curve, such as endpoint terminal, convex hull, symmetry, and geometric invariance. Then, the idea of the quintic trigonometric Bézier curve is extended to construct different surfaces such as tensor

product, swept surface, swung surface, and ruled surface. This section also introduces the Gaussian curvature, mean curvature, and curvature colour mapping methods.

Quintic Trigonometric Bézier Curve

Quintic trigonometric Bézier curves with two shape parameters are introduced by Misro et al. (2017), indicating that the shape parameters can permit flexibility on the curve's shape aside from describing the curve's geometrical characteristics. In addition, geometric characteristics can maintain the curve's shape by adjusting the parameters' values, in which altering the control points can make it more convenient. For example, quintic trigonometric Bézier curve with two shape parameters and six control points Pi, i=0,1,2,3,4,5 in $\mathbb{R}^2$ or $\mathbb{R}^3$ is defined as Equation 1:

$$z(t) = \sum_{i=0}^{5} P_i f_i(t), \qquad t \in [0,1], \qquad \alpha, \beta \in [-4,1]. \tag{1}$$

The quintic trigonometric Bézier basis functions for arbitrarily real values of shape parameters α and β, where $-4 \leq \alpha, \beta \leq 1$, and for $t \in [0,1]$ are given as Equation 2:

$$\begin{aligned}
f_0(t) &= \left(1-\sin\frac{\pi t}{2}\right)^4 \left(1-\alpha\sin\frac{\pi t}{2}\right),\\
f_1(t) &= \sin\frac{\pi t}{2}\left(1-\sin\frac{\pi t}{2}\right)^3 \left(4+\alpha-\alpha\sin\frac{\pi t}{2}\right),\\
f_2(t) &= \left(1-\sin\frac{\pi t}{2}\right)^2 \left(1-\cos\frac{\pi t}{2}\right)\left(8\sin\frac{\pi t}{2}+3\cos\frac{\pi t}{2}+9\right),\\
f_3(t) &= \left(1-\cos\frac{\pi t}{2}\right)^2 \left(1-\sin\frac{\pi t}{2}\right)\left(8\cos\frac{\pi t}{2}+3\sin\frac{\pi t}{2}+9\right),\\
f_4(t) &= \cos\frac{\pi t}{2}\left(1-\cos\frac{\pi t}{2}\right)^3 \left(4+\beta-\beta\cos\frac{\pi t}{2}\right),\\
f_5(t) &= \left(1-\cos\frac{\pi t}{2}\right)^4 \left(1-\beta\cos\frac{\pi t}{2}\right),
\end{aligned} \tag{2}$$

where f_i is the basis functions and P_i is the control points for the quintic trigonometric Bézier with i=0,1,2,3,4,5 in $\mathbb{R}^2$ or $\mathbb{R}^3$ as shown in Figure 1.

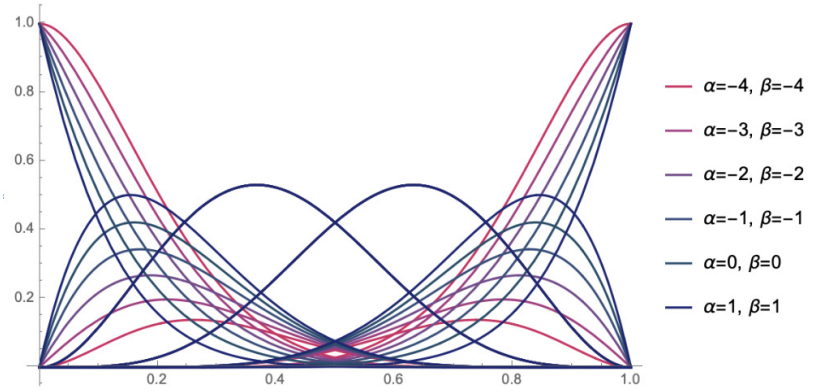

Figure 1. The quintic trigonometric Bézier polynomial basis functions

Endpoint Terminal. The endpoint terminal or curve's endpoints are represented by the first and last control points, which can be defined as Equation 3:

$$\begin{aligned} z(0) &= P_0 \\ z(1) &= P_5 \\ z'(0) &= -\frac{\pi}{2}(P_0 - P_1)(4+\alpha) \\ z'(1) &= -\frac{\pi}{2}(P_4 - P_5)(4+\beta) \\ z''(0) &= \pi^2\big(3P_2 - 2P_1(3+\alpha) + P_0(3+2\alpha)\big) \\ z''(1) &= \pi^2\big(3P_3 - 2P_4(3+\beta) + P_5(3+2\beta)\big) \end{aligned} \tag{3}$$

Convex Hull. Convex hull property for the quintic trigonometric Bézier curve for a given point P_i, where i=0,1,2,3,4,5 in $\mathbb{R}^2$ or $\mathbb{R}^3$, must lie inside its control point polygon as demonstrated in Figure 2. Therefore, a complete trigonometric Bézier curve segment must contain within its control polygon, spanned by space P_0, P_1, P_2,P_3, P_4, and P_5.

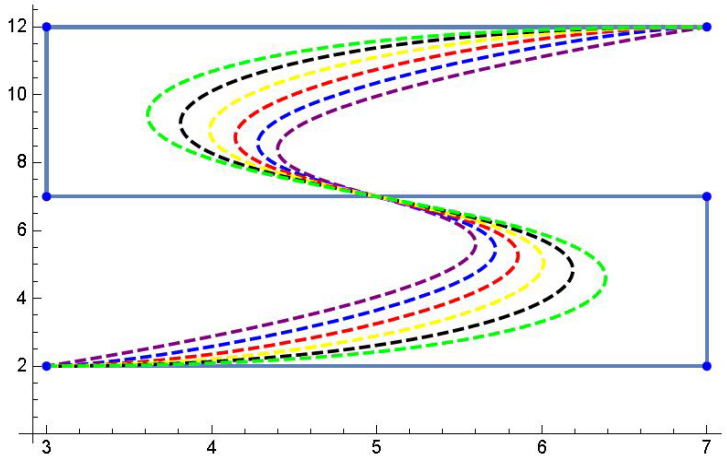

Figure 2. The quintic trigonometric Bézier curve's projection inside the convex hull

Symmetry. The identical Bézier curve shape will be produced if the control points are defined in the opposite order. To be specific, $\{P_5, P_4, P_3, P_2, P_1, P_0\}$ and $\{P_0, P_1, P_2, P_3, P_4, P_5\}$ define the same quintic trigonometric Bézier curve in distinct parameterisation Equation 4:

$$z(t;\, \alpha, \beta{:}P_0, P_1, P_2, P_3, P_4, P_5) = z(1-t;\, \alpha, \beta{:}\, P_5, P_4, P_3, P_2, P_1, P_0) \tag{4}$$

with $-4 \le \alpha, \beta \le 1$ and $0 \le t < 1$.

Geometric Invariance. Geometric invariance is another property of the quintic trigonometric Bézier curve that remains unchanged when its control points are rotated and translated. Thus, the curve's shape is independent of the coordinate system used, which fulfils Equations 5 and 6:

$$z(t;\ \alpha,\beta:\ P_0+m,P_1+m,P_2+m,P_3+m,P_4+m,P_5+m) = z(t;\ \alpha,\beta:P_0,P_1,P_2,P_3,P_4,P_5)+m \tag{5}$$

$$z(t;\ \alpha,\beta:P_0*T,P_1*T,P_2*T,P_3*T,P_4*T,P_5*T) = z(t;\ \alpha,\beta:P_0,P_1,P_2,P_3,P_4,P_5)*T \tag{6}$$

where $0 \le t \le 1, -4 \le \alpha,\beta \le 1$, m is an arbitrary vector in $\mathbb{R}^2$ or $\mathbb{R}^3$, while T is an arbitrary $d \times d$ matrix with d = 5 or 6 depending on the initial value of i.

Quintic Trigonometric Bézier Surface

A construction of quintic trigonometric Bézier surface, as mentioned by Ammad and Misro (2020), can be expressed mathematically as Equation 7:

$$S(u,v,\alpha_1,\beta_1,\alpha_2,\beta_2) = \sum_{i=0}^{m}\sum_{j=0}^{n} f_{i,m}(u)f_{j,n}(v)P_{i,j}, \tag{7}$$

where $P_{i,j} \in \mathbb{R}^3 (i = 0,1,2,\dots,m; j = 0,1,2,\dots.n)$ are the control points with degree m and n. This surface with domain $(u,v) \in [0,1] \times [0,1]$, also has the shape parameters α_1,β_1 and α_2,β_2 of the basis functions $f_{i,m}(u)$ and $f_{j,n}(v)$, respectively.

Note that swept, ruled, and swung surfaces are some examples of advanced surface construction techniques typically available in CAD. Furthermore, the CAD-generated surfaces are the tensor product's representation of the biquintic trigonometric Bézier surface.

Tensor-Product Surface. One of the essential approaches to construct a surface on a rectangular domain is tensor-product surfaces. For instance, the biquintic trigonometric Bézier surface is generated using the same Equation 7 with the same degree, where m=n=5. In addition, four shape parameters $(\alpha_1,\beta_1,\alpha_2,\beta_2)$ and 36 control points are required to generate this surface. Here, the range of the parameters is between -4 to 1 for both u and v directions.

Swept Surface. A swept surface can be developed from the basic idea of the biquintic trigonometric Bézier surface. As demonstrated in Figure 3, the surface is created by moving the section curve along the trajectory curve. A cylindrical surface is also formed when the sweep surface's path curve is straight. However, Chang (2016) claimed that the generated sweep surface is a revolution's surface if the path curve is a circular arc. As a result, all revolving and cylindrical surfaces are characterised as unique examples of sweep surfaces.

Let $G_1(u)$ be the path curve with shape parameters α_1, β_1 and $G_2(v)$ be the trajectory curve with α_2, β_2 as the shape parameters. Then, both curves produce Equation 8:

$$G_1(u,\alpha_1,\beta_1) = \sum_{j=0}^{m} f_{i,m}(u)p_{i,m}\ , \quad u \in [0,1],$$
$$G_2(v,\alpha_2,\beta_2) = \sum_{j=0}^{n} f_{j,n}(v)q_{j,n}\ , \quad v \in [0,1]. \tag{8}$$

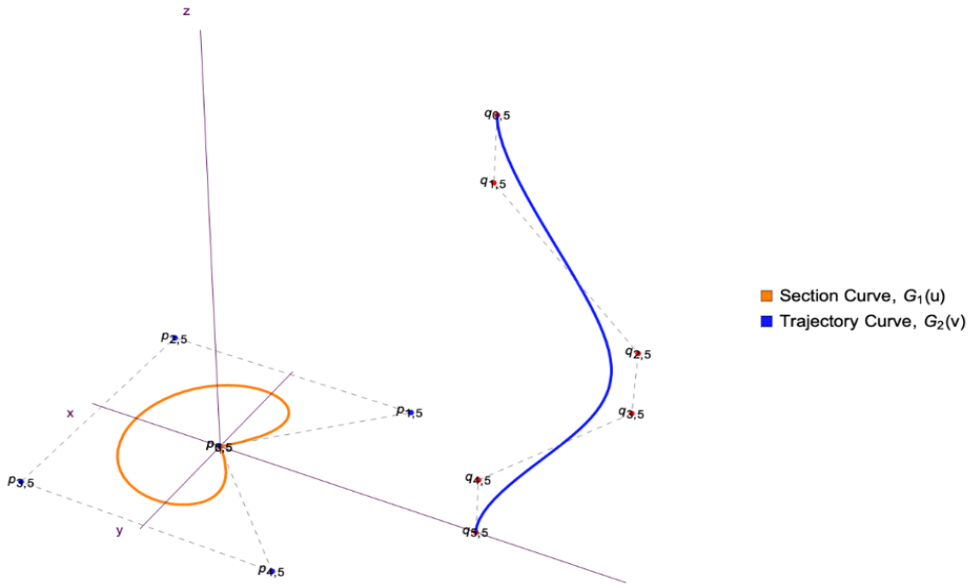

Figure 3. The construction of a swept surface using trajectory curve and section curve

Then, the general equation of the swept surface based on Ammad and Misro (2020) as Equation 9:

$$S_{swept}(u,v,\alpha_1,\beta_1,\alpha_2,\beta_2) = M(v)G_1(u) + G_2(v). \tag{9}$$

$M(v)$ is a 3×3 dimensional matrix of function v, representing an identity matrix. Consequently, the general expression can be expressed as Equation 10:

$$S_{swept}(u, v, \alpha_1, \beta_1, \alpha_2, \beta_2) = G_1(u) + G_2(v). \quad (10)$$

Using control points $p_{-i,j}$ and shape parameters from Equation 10, a swept surface with $(u, v) \in [0,1] \times [0,1]$ can be constructed as Equation 11:

$$S_{swept}(u, v, \alpha_1, \beta_1, \alpha_2, \beta_2) = \sum_{j=0}^{m} \sum_{j=0}^{n} f_{i,m}(u)\ f_{j,n}(v) p_{i,j}. \quad (11)$$

Swung Surface. According to Piegl and Tiller (1996), a swung surface is a generalisation of a surface revolution. Hu et al. (2018) stated that the profile curve is swung along an axis to create this type of surface, as shown in Figure 4. Assuming that Equation 8 is the profile curve and trajectory curve in the *xz* and *xy*-plane, respectively, with the control points, $p_{i,m} = \left(p_{i,m}^x, 0, p_{i,m}^z\right)$ and $q_{-j,n} = \left(q_{j,n}^x, q_{j,n}^y, 0\right)$, where $(i = 0, 1, 2, \ldots, m; j = 0, 1, 2, \ldots . n)$. Then, the formal definition of the swung surface with $(u, v) \in [0,1] \times [0,1]$ is defined as Equation 12:

$$S_{swung}(u, v, \alpha_1, \beta_1, \alpha_2, \beta_2) = \sum_{i=0}^{m} \sum_{j=0}^{n} f_{i,m}(u)\ f_{j,n}(v) p_{i,j}, \quad (12)$$

where the control points, $p_{i,j} = \left(\lambda f_m^x(u) f_n^x(v), \lambda f_m^x(u) f_n^y(v), f_m^z(u)\right)$ and $\lambda(\lambda > 0)$ is the scaling factor.

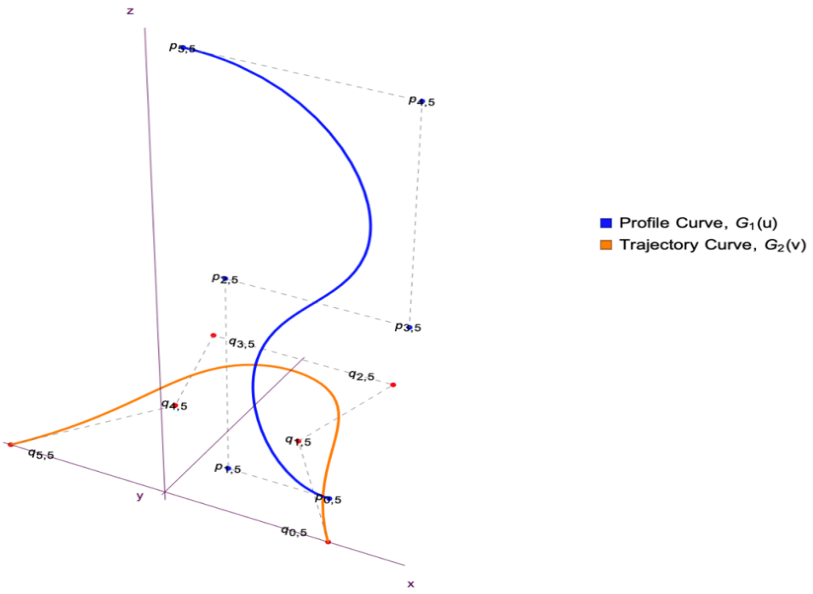

Figure 4. The construction of a swung surface using profile curve and trajectory curve

Ruled Surface. The representation of the quintic trigonometric Bézier surface can be enhanced to a ruled surface. A surface is called a ruled surface if the two opposite curves that are not necessarily straight lines are generated by a generator or ruling in a straight-line motion. Let $P(u)$ and $Q(u)$ be the two directrices of curves in u-direction, while $R(u)$ is the ruling line. Then, the parametric representation of the ruled surface, $C(u,v)$, is given by Equation 13:

$$C(u,v) = P(u) + vR(u). \tag{13}$$

If $R(u) = Q(u) - P(u)$, the equation is then extended to a quintic trigonometric Bézier (Equation 14):

$$\begin{aligned} P(u,\alpha_1,\beta_1) &= \textstyle\sum_{i=0}^{m} f_{i,m}(u)p_{i,m}\,, \quad u \in [0,1], \\ Q(u,\alpha_1,\beta_1) &= \textstyle\sum_{i=0}^{m} f_{i,m}(u)q_{i,m}\,, \quad u \in [0,1]. \end{aligned} \tag{14}$$

These imply that $R(u,\alpha_1,\beta_1) = Q(u,\alpha_1,\beta_1) - P(u,\alpha_1,\beta_1)$. As a result, the general equation with respect to the ruled surface concerning the tensor product of biquintic trigonometric Bézier surface is given by Equation 15:

$$S_{Ruled}(u,v,\alpha_1,\beta_1,\alpha_2,\beta_2) = P(u,\alpha_1,\beta_1) + vR(u,\alpha_1,\beta_1), \tag{15}$$

where $(u,v) \in [0,1] \times [0,1]$.

Curvature and Surface Curvature

Curvature is a measure of how sharply a curve bend. The curve's curvature is a measurement of the rate it shifts direction at a particular location. There are various formulas for calculating a curve's curvature. The basic definition is as Equation 16:

$$\kappa = \left\| \frac{d\vec{T}}{ds} \right\| \tag{16}$$

where s is the arc length and $\vec{T}$ is the unit tangent. Equation 16 only can be used to calculate the curve's curvature, where the equation needs to be extended to evaluate surface curvature. Therefore, several approaches must be applied to calculate the curvature of a surface. The classical differential geometry concepts of the first and second fundamental forms are commonly used to determine the Gaussian and mean curvature of a surface. Based on Pressley (2010), Beck et al. (1986) and Farin et al. (2002), the first fundamental form that can be derived from Equation 7 is given by Equations 17 and 18:

$$ds^2 = Edu^2 + 2Fdudv + Gdv^2 \tag{17}$$

where

$$\begin{aligned} E &= S_u(u, v, \alpha_1, \beta_1, \alpha_2, \beta_2) \cdot S_u(u, v, \alpha_1, \beta_1, \alpha_2, \beta_2), \\ F &= S_u(u, v, \alpha_1, \beta_1, \alpha_2, \beta_2) \cdot S_v(u, v, \alpha_1, \beta_1, \alpha_2, \beta_2), \\ G &= S_v(u, v, \alpha_1, \beta_1, \alpha_2, \beta_2) \cdot S_v(u, v, \alpha_1, \beta_1, \alpha_2, \beta_2). \end{aligned} \tag{18}$$

Then, the equation for the second fundamental form is given by Equations 19 and 20:

$$dh^2 = Ldu^2 + 2Mdudv + Ndv^2 \tag{19}$$

where

$$\begin{aligned} L &= S_{uu}(u, v, \alpha_1, \beta_1, \alpha_2, \beta_2) \cdot \boldsymbol{n}, \\ M &= S_{uv}(u, v, \alpha_1, \beta_1, \alpha_2, \beta_2) \cdot \boldsymbol{n}, \\ N &= S_{vv}(u, v, \alpha_1, \beta_1, \alpha_2, \beta_2) \cdot \boldsymbol{n}, \end{aligned} \tag{20}$$

in which the unit surface normal, $\boldsymbol{n}$ is as Equation 21:

$$\boldsymbol{n} = \frac{S_u(u, v, \alpha_1, \beta_1, \alpha_2, \beta_2) \times S_v(u, v, \alpha_1, \beta_1, \alpha_2, \beta_2)}{\| S_u(u, v, \alpha_1, \beta_1, \alpha_2, \beta_2) \times S_v(u, v, \alpha_1, \beta_1, \alpha_2, \beta_2) \|}. \tag{21}$$

Gaussian Curvature. Gaussian curvature, K is a product of the principal curvatures, $K = k_1k_2$. This curvature depends on the first and second fundamental form coefficients, which can also be expressed in E, F and G and their derivatives. The value K depends only on the intrinsic geometry of the surface. It implies that if the surface is deformed, it does not alter its length measurement (Farin et al., 2002). The Gaussian curvature may carry the property that helps evaluate the surface, which can be a saddle, convex and concave. If the surface shape resembles a saddle, one of the main curvatures is positive, and the other is negative. Both principal curvatures are negative for the convex surface, while the main curvatures are positive if the surface is concave. The formula for the Gaussian curvature is given by Equation 22:

$$K = \frac{LN - M^2}{EG - F^2}. \tag{22}$$

Mean Curvature. The mean curvature of a surface, H, is an extrinsic curvature measure in differential geometry describing the curvature of an embedded surface locally in a region of space such as Euclidean space. The coefficients of the first and second fundamental forms can also be used to express mean curvature. It resembles the average of the principal

curvatures, $H = \frac{1}{2}(\kappa_1 + \kappa_2)$. If $H = 0$, the result yields minimal surface. Then, the alternative formula for the mean curvature is as Equation 23:

$$H = \frac{EN - 2FM + GL}{2(EG - F^2)} . \quad (23)$$

Curvature Colour Mapping

There are several methods for visualising surface curvature that has been investigated. Surface analysis, also known as interrogation, is a crucial component of CAD and computer graphics in detecting surface flaws and visualising a surface (Hahmann, 1999). This method can analyse the geometry surface features such as curvature. Normal vectors, contour lines and colour-coded mapping are three of the most widely utilised methods (Seidenberg et al., 1992). Previously, Dill (1981) tested the curvature colour mapping on 1980 Pontiac and Oldsmobile automotive components, which are body hood and front fender, respectively, to inspect their smoothness. Besides, as Gatzke et al. (2005) claimed, curvature maps are useful for distinguishing local shapes and finding their corresponding shape similarity in the shape matching problem. Thus, the curvature colour mapping technique has been chosen to analyse the Gaussian and mean curvature. A colour-coded map is applied on the surface to visualise and interpret the curvature. This research applies the colour mapping method on the Gaussian and mean curvature plots of different surfaces with fixed shape parameters (-4, -4, 1, 1) in Wolfram Mathematica. The bar legends are generated for each plot to identify the range of curvature values.

RESULT AND DISCUSSION

The findings of this research are presented and discussed in this section. This discussion focuses on the curvature analysis of the surfaces by determining a point on a surface's local geometry and the surface types based on the mean and Gaussian curvature signs.

Curvature Analysis

The curvature of a surface can be calculated in a variety of ways. However, this research focuses on the Gaussian and mean curvature. The first and second fundamental forms of a surface patch are used to compute the curvature of the surface. The product of the principal curvatures determines the surface's Gaussian curvature. Every positive Gaussian curvature point has its tangent plane touch the surface at a single point, whereas a point that is negative Gaussian curvature has its tangent plane cut the surface (Oxman, 2007). Negative or zero Gaussian curvature can be found at any place with zero mean curvature. The interpretation of Gaussian curvature is less clear, but it can be figured out by looking at surfaces with different Gaussian curvatures (Devaraj, 2020).

The half of the sum of the principal curvatures at a point indicates the surface's mean curvature at that particular point. Surfaces that have a zero mean curvature is known as minimum surfaces. Thus, a minimal surface is the subset of constant mean curvature surfaces where the curvature is zero (Oxman, 2007). In order to analyse the surface curvature, the value of minimum principal curvature, k_{min} and maximum principal curvature, k_{max} need to be considered. Both formulas are shown as Equation 24:

$$\kappa_{max} = H + \sqrt{H^2 - K}, \\ \kappa_{min} = H - \sqrt{H^2 - K}. \tag{24}$$

Based on Marsh (2005), all the essential theories in differential geometry can be used to determine the local geometry of a surface, as shown in Table 1.

Table 1
Surface's local geometry at a point

Types of Points	Property of K and H	Sign of k_{min} and k_{max}
Parabolic Point	$K = 0, H \neq 0$	k_{min} or $k_{max} = 0$
Hyperbolic Point	$K < 0, H \neq 0$	Have opposite signs
Elliptic Point	$K > 0, H \neq 0$	Have the same signs

Informally, an elliptic point curve for all directions, in the same way, has the same principal curvature sign. On the other hand, a hyperbolic point is like a saddle point because the principal curvatures are of opposite signs. Meanwhile, a parabolic point has a positive principal curvature since the surface is non-planar but achieves a minimum curvature of zero in some directions. Thus, a surface around a parabolic point is like a curved piece of paper, where a surface seems to be flat around a planar point.

Table 2
Type of surfaces from mean and Gaussian curvature signs

	$K < 0$	$K = 0$	$K > 0$
$H < 0$	saddle ridge	ridge	peak
$H = 0$	minimal surface	flat	not possible
$H > 0$	saddle valley	valley	pit

According to Besl (2012), the Gaussian and mean curvature signs can determine basic types of surfaces. Both curvatures produce eight different types of surfaces, as shown in Table 2 and explained in Figure 5.

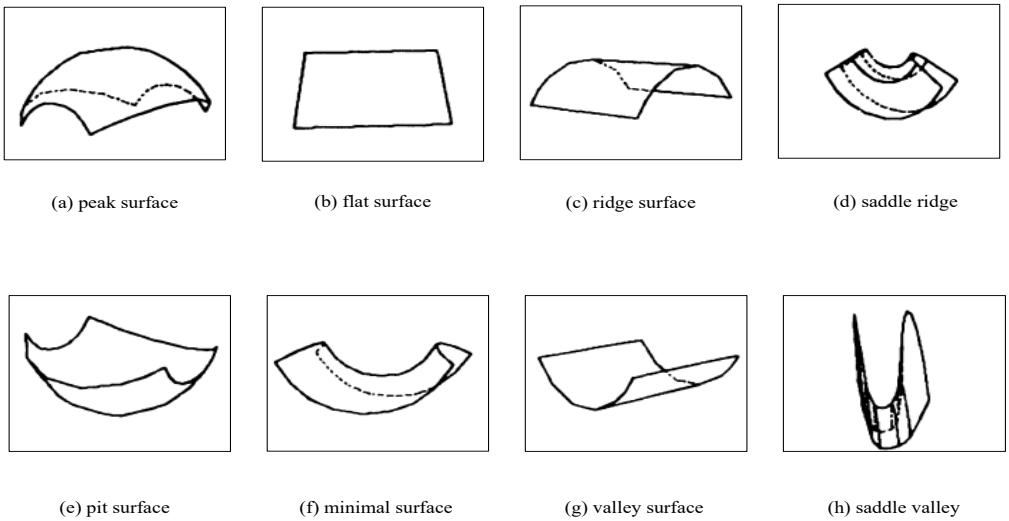

Figure 5. The eight visible-invariant *HK*-sign surface types [Source: Besl (2012)]

Tensor-Product Surface. Based on Figure 6a, most points of the tensor-product surface are hyperbolic points since $H \neq 0$ and $K < 0$. Moreover, at a hyperbolic point, k_{min} and k_{max} have opposite signs, giving the surface a saddle shape. Parabolic points are obtained when, either point k_{min} or k_{max} equals zero, as shown in Table 3. As a result, the surface has a parabolic cylinder structure, and it is linear in one principal direction. The surface is referred to as a trough or a ridge in computer graphic applications. The elliptic point is obtained at $H \neq 0$ and $K > 0$. Moreover, the signs k_{min} and k_{max} are the same.

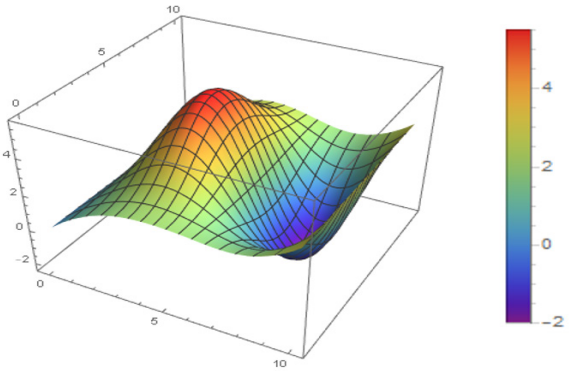

(a) Tensor product

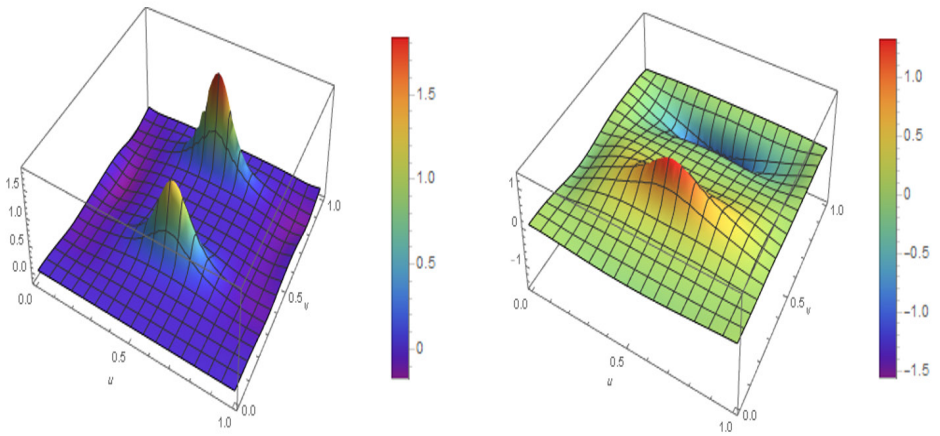

(b) Gaussian curvature (c) Mean curvature

Figure 6. 3D plot of the tensor-product surface with shape parameters (-4, -4, 1, 1)

Table 3

Parabolic points on tensor-product surface

u	v	K	H	k_{min}	k_{max}
0	0	0.0000	0.0424	0.0000	0.0849
0.1	0	0.0000	0.0224	0.0000	0.0448
0.2	0	0.0000	-0.0193	-0.0387	0.0000
0.3	0	0.0000	-0.0614	-0.1228	0.0000
0.4	0	0.0000	-0.0914	-0.1828	0.0000
0.5	0	0.0000	-0.1039	-0.2079	0.0000
0.6	0	0.0000	-0.0983	-0.1967	0.0000
0.7	0	0.0000	-0.0765	-0.1530	0.0000
0.8	0	0.0000	-0.0429	-0.0859	0.0000
0.9	0	0.0000	-0.0060	-0.0119	0.0000
1.0	0	0.0000	0.0212	0.0000	0.0424

By referring to Table 4, the points are (0.3, 0.3), (0.3, 0.4), (0.4, 0.2), (0.4, 0.3), (0.4, 0.4), (0.4, 0.5), (0.5, 0.2), (0.5, 0.3), (0.5, 0.4), (0.5, 0.5), (0.5, 0.6), (0.6, 0.2), (0.6, 0.3), (0.6, 0.4), (0.6, 0.5), (0.7, 0.3) and (0.7, 0.4) for the positive sign. Meanwhile, for the negative sign, the points are (0.3, 0.8), (0.3, 0.9), (0.4, 0.7), (0.4, 0.8), (0.4, 0.9), (0.5, 0.7), (0.5, 0.8), (0.5, 0.9), (0.6, 0.7), (0.6, 0.8), (0.6, 0.9), (0.7, 0.8) and (0.7, 0.9), as shown in Table 5. As a result, the normal sections have the same profile, indicating the shape of an ellipsoid.

Based on Figure 5, there are two prominent basic surface shapes in Figure 6a. The red colour is a peak surface, which means the surface bulges in the direction opposite to the normal surface, while the blue colour represents the pit surface shape. According to Table 2, peak and pit surface have $K > 0$ but with different mean curvature values, which are $H < 0$ and $H > 0$, respectively. It can be validated from Figure 6b, where the Gaussian curvature is less than zero, and the colour is blue. Meanwhile, the mean curvature plot in Figure 6c shows two regions with positive and negative curvature values.

Table 4

Positive elliptic points on tensor-product surface

u	v	K	H	k_{min}	k_{max}
0.3	0.3	0.0516	0.4150	0.0678	0.7622
0.3	0.4	0.0728	0.5082	0.0775	0.9390
0.4	0.2	0.0069	0.1554	0.0241	0.2866
0.4	0.3	0.2211	0.5616	0.2546	0.8686
0.4	0.4	0.3393	0.7234	0.2945	1.1523
0.4	0.5	0.0178	0.1900	0.0546	0.3254
0.5	0.2	0.0113	0.1367	0.0510	0.2223
0.5	0.3	0.3588	0.6097	0.4962	0.7231
0.5	0.4	0.6049	0.8251	0.5495	1.1007
0.5	0.5	0.0225	0.1566	0.1117	0.2014
0.5	0.6	0.0003	0.0184	0.0114	0.0255
0.6	0.2	0.0083	0.1321	0.0366	0.2276
0.6	0.3	0.2568	0.5623	0.3186	0.8061
0.6	0.4	0.4233	0.7625	0.3648	1.1601
0.6	0.5	0.0176	0.1606	0.0704	0.2508
0.7	0.3	0.0823	0.4499	0.1034	0.7963
0.7	0.4	0.1245	0.5931	0.1164	1.0698

Table 5

Negative elliptic points on tensor-product surface

u	v	K	H	k_{min}	k_{max}
0.3	0.8	0.0780	-0.5509	-1.0258	-0.0761
0.3	0.9	0.0404	-0.3854	-0.7143	-0.0566

Table 5 *(Continue)*

u	v	K	H	k_{min}	k_{max}
0.4	0.7	0.0032	-0.1057	-0.1950	-0.0165
0.4	0.8	0.2649	-0.6267	-0.9843	-0.2692
0.4	0.9	0.1084	-0.3906	-0.6009	-0.1804
0.5	0.7	0.0067	-0.0925	-0.1355	-0.0495
0.5	0.8	0.3731	-0.6235	-0.7484	-0.4985
0.5	0.9	0.1383	-0.3719	-0.3783	-0.3655
0.6	0.7	0.0043	-0.1060	-0.1892	-0.0228
0.6	0.8	0.2595	-0.6174	-0.9662	-0.2686
0.6	0.9	0.1089	-0.3924	-0.6046	-0.1802
0.7	0.8	0.0779	-0.5432	-1.0092	-0.0772
0.7	0.9	0.0408	-0.3893	-0.7221	-0.0565

Swept Surface. The swept surface is in Figure 7a, where the parabolic point occurs when $H \neq 0$ and $K = 0$. Thus, by referring to Table 1, either k_{min} and k_{max} are equal to zero. Therefore, the surface assumes to be in the form of a parabolic cylinder, and this surface can be characterised as a ridge or a trough. The points are from (0.5, 0) until (0.5, 1), as demonstrated in Table 6. The elliptic point is at $H \neq 0$ and $K > 0$, where the sign of k_{min} and k_{max} are the same.

As a result, the normal sections have the same profile, implying an ellipsoid form. The points are given by (0, 0) until (0, 2), (0, 0.8) until (0.1, 0.2), (0.1, 0.8) until (0.2, 0.2), (0.2, 0.8) until (0.3, 0.2), (0.3, 0.8) until (0.3, 1), (0.4, 0.3) until (0.4, 0.7), (0.6, 0) until (0.6, 0.2), (0.6, 0.8) until (0.6, 1), (0.7, 0.3) until (0.7, 0.7), (0.8, 0.3) until (0.8, 0.7), (0.9, 0.3) until (0.9, 0.7) and (1, 0.3) until (1, 0.7). Then, the remaining points on the swept surface are hyperbolic points, where $H \neq 0$ and $K < 0$. At the hyperbolic point, k_{min} and k_{max} have opposite signs, implying a saddle shape.

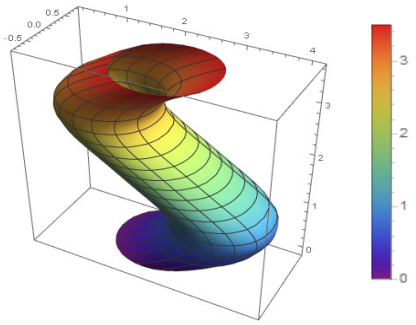

(a) Swept surface

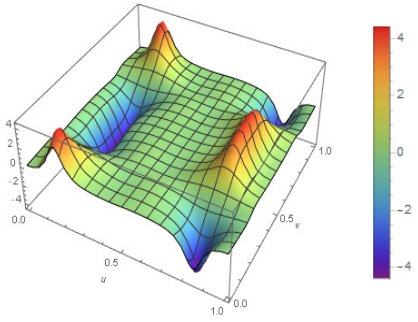

(b) Gaussian curvature

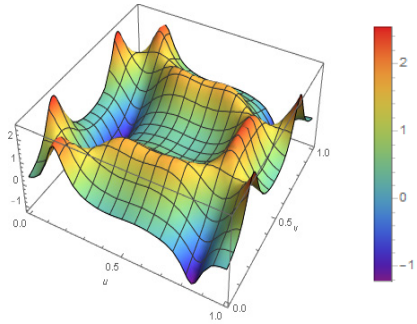

(c) Mean curvature

Figure 7. 3D plot of the swept surface with shape parameters (-4, -4, 1, 1)

Table 6

Parabolic points on a swept surface

u	v	K	H	k_{min}	k_{max}
0.5	0	0.0000	0.2642	0.0000	0.5284
0.5	0.1	0.0000	0.7666	0.0000	1.5333
0.5	0.2	0.0000	1.5630	0.0000	3.1260
0.5	0.3	0.0000	1.2224	0.0000	2.4449
0.5	0.4	0.0000	0.5065	0.0000	1.0131
0.5	0.5	0.0000	0.3403	0.0000	0.6806
0.5	0.6	0.0000	0.5065	0.0000	1.0131
0.5	0.7	0.0000	1.2224	0.0000	2.4449
0.5	0.8	0.0000	1.5630	0.0000	3.1260
0.5	0.9	0.0000	0.7666	0.0000	1.5333
0.5	1.0	0.0000	0.2642	0.0000	0.5284

Based on the observation, Figure 7a has two prominent basic surface shapes. The left of the swept surface is possibly a ridged surface, implying that a line of curvature has a local maximum and minimum of principal curvature. In contrast, the right side of the surface would have a valley shape. Based on Table 2, ridge and valley shapes have $K = 0$ but with different mean curvature values of $H < 0$ and $H > 0$, respectively. The Gaussian curvature plot in Figure 7b demonstrated the two regions with positive and negative curvature values. Roughly, the mean curvature plot in Figure 7c shows positive value regions. Therefore, if comparisons are made from Figures 7b and 7c, some pit surface, valley surface, saddle surface, and saddle ridge surface exist.

Swung Surface. Figure 8a portrays a swung surface. At point (0, 0) until (0.4, 1), k_{min} and k_{max} have the same sign, implying an elliptic point. As a result, the normal sections have the same profile, indicating an ellipsoid form. Meanwhile, at points (0.5, 0) until (1, 1), the signs are opposite, implying hyperbolic points. As a result, the surface has a saddle form. However, at points (0, 1), (0.1, 1), (0.2, 1), (0.3, 1), (0.4, 1), (0.5, 1), (0.6, 1), (0.7, 1), (0.8, 1), (0.9, 1), (1, 1) and (1, 0.9), either k_{min} and k_{max} equal to zero by referring to Table 7. Therefore, the surface is a parabolic point. As a result, the surface has a parabolic cylinder shape and is linear in one principal direction.

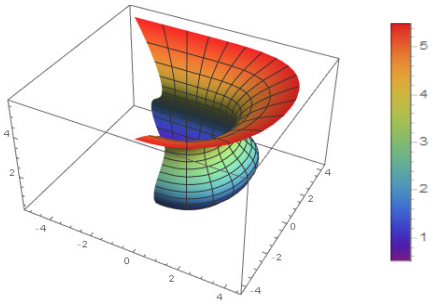

(a) Swung surface

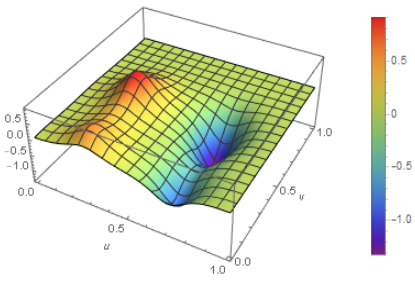

(b) Gaussian curvature

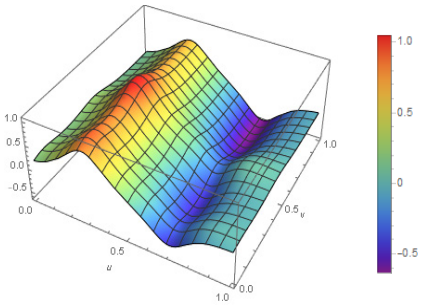

(c) Mean curvature

Figure 8. 3D plot of the swung surface with shape parameters (-4, -4, 1, 1)

Table 7

Parabolic points on a swung surface

u	v	K	H	k_{min}	k_{max}
0	1.0	0.0000	0.0822	0.0000	0.1644
0.1	1.0	0.0000	0.2272	0.0000	0.4544
0.2	1.0	0.0000	0.5225	0.0000	1.0451
0.3	1.0	0.0000	0.6398	0.0000	1.2795
0.4	1.0	0.0000	0.3093	0.0000	0.6185
0.5	1.0	0.0000	-0.0103	-0.0206	0.0000
0.6	1.0	0.0000	-0.3487	-0.6973	0.0000
0.7	1.0	0.0000	-0.6418	-1.2835	0.0000
0.8	1.0	0.0000	-0.3785	-0.7570	0.0000
0.9	1.0	0.0000	-0.1321	-0.2641	0.0000
1.0	1.0	0.0000	-0.0461	-0.0922	0.0000

Based on inspection in Figure 8a, there exist some basic surface shapes. For example, the red-yellow region has a pit surface shape, the green-blue and blue colour has a peak surface shape. Roughly, the shape of the swung surface has a saddle ridge on the top of the surface, while the bottom of the surface has a ridge type of surface, with the middle region having a valley surface. As a result, in Figures 8b and 8c, the Gaussian and mean curvature plot justifies the inspection of the swung surface.

Ruled Surface. We assume sweeping out a surface by moving a line. Such a surface is known as a ruled surface. Figure 9a demonstrates the ruled surface with shape parameters (-4, -4, 1, 1). There are several methods for calculating a surface's curvature. The result of a ruled surface is that all the points on the surface are hyperbolic points, where the equivalent k_{min} and k_{max} have opposite signs.

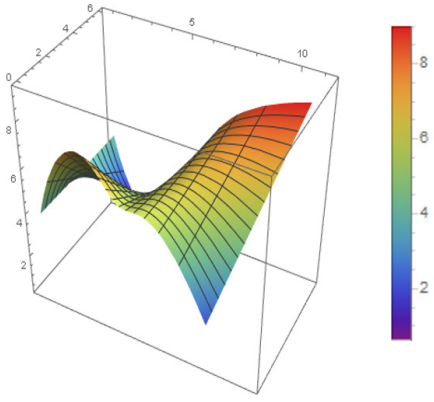

(a) Ruled surface

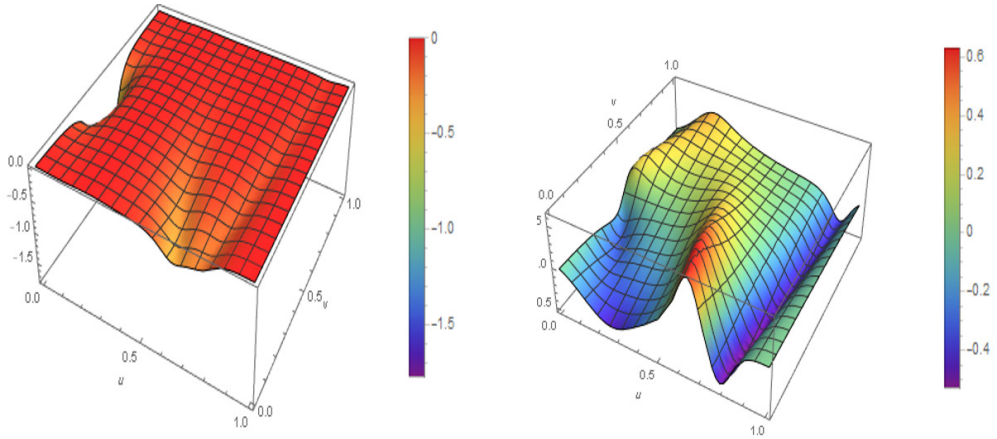

(b) Gaussian curvature (c) Mean curvature

Figure 9. 3D plot of the ruled surface with shape parameters (-4, -4, 1, 1)

Table 8

The minimal surface at a point of the ruled surface

u	v	K	H	k_{min}	k_{max}
0	0.5	-1.7778	0.0000	-1.3333	1.3333

Based on Figure 5, there are notably basic surface shapes in Figure 9a: saddle ridge surface and saddle valley surface region. Moreover, Figure 9a resembles a minimal surface shape, and there is a point on the surface with zero mean curvature, as shown in Table 8. The saddle ridge and valley surface can be verified based on Figure 9b, where most Gaussian curvature plots are less than zero. Meanwhile, the mean curvature plot in Figure 9c shows two regions with positive, negative and some areas with approximately zero curvature values.

CONCLUSION

This work highly focuses on the Gaussian and mean curvature of different surfaces, such as tensor-product, swept, swung, and ruled surfaces. The Gaussian and mean curvature of the surfaces are calculated, and the curvatures are represented using a 3D plot with a colour-coded map default in Wolfram Mathematica. By visualising surface curvature, the geometric shape of surfaces can be determined and analysed.

Nevertheless, the curvature plots have not been mapped on the surface. Thus, it is not easy to inspect the Gaussian and mean curvature on the specific region. Moreover, the

rainbow colours used are difficult to differentiate and detect the slight changes in curvature values because most of the calculated curvature values are relative to zero curvatures. Besides, the range scales of all the bar legends are also insensitive due to decimal places being rounded off.

There are a few suggestions that can be made for future works. First, this work can be extended to determine the effect of a surface when a different set of shape parameters are used. In addition, shape index-curvedness of curvature (SC curvature) can also be another alternative to measure and represent curvature analysis of surfaces.

ACKNOWLEDGEMENT

The Ministry of Higher Education Malaysia supported this research through the Fundamental Grant Scheme (FRGS/1/2020/STG06/USM/03/1) and the School of Mathematical Sciences, Universiti Sains Malaysia. In addition, the authors are very grateful to the anonymous referees for their valuable suggestions.

REFERENCES

Adnan, S. B. Z., Ariffin, A. A. M., & Misro, M. Y. (2020). Curve fitting using quintic trigonometric Bézier curve. In *AIP Conference Proceedings* (Vol. 2266, No. 1, p. 040009). AIP Publishing LLC. https://doi.org/10.1063/5.0018099

Ammad, M., & Misro, M. Y. (2020). Construction of local shape adjustable surfaces using quintic trigonometric Bézier curve. *Symmetry*, *12*(8), Article 1205. https://doi.org/10.3390/sym12081205

Ammad, M., Misro, M. Y., & Ramli, A. (2022). A novel generalized trigonometric Bézier curve: Properties, continuity conditions and applications to the curve modeling. *Mathematics and Computers in Simulation*, *19*, 744-763. https://doi.org/10.1016/j.matcom.2021.12.011

Bartkowiak, T., & Brown, C. A. (2019). Multiscale 3D curvature analysis of processed surface textures of aluminum alloy 6061 T6. *Materials*, *12*(2), Article 257. https://doi.org/10.3390/ma12020257

Beck, J. M., Farouki, R. T., & Hinds, J. K. (1986). Surface analysis methods. *IEEE Computer Graphics and Applications*, *6*(12), 18-36. https://doi.org/10.1109/MCG.1986.276587

Besl, P. J. (2012). *Surfaces in range image understanding*. Springer Science & Business Media.

Bibi, S., Abbas, M., Misro, M. Y., Majeed, A., & Nazir, T. (2021). Construction of generalized hybrid trigonometric Bézier surfaces with shape parameters and their applications. *Journal of Mathematical Imaging and Vision*, *63*(9), 1118-1142. https://doi.org/10.1007/s10851-021-01046-y

Chang, K. H. (2016). *e-Design: computer-aided engineering design*. Academic Press.

Chen, Q., & Wang, G. (2003). A class of Bézier-like curves. *Computer Aided Geometric Design*, *20*(1), 29-39. https://doi.org/10.1016/S0167-8396(03)00003-7

Devaraj, A. (2020). *An overview of curvature*. Retrieved May 5, 2021, from https://web.ma.utexas.edu/users/drp/files/Spring2020Projects/DRP_spring2020_final%20-%20Ashwin%20Devaraj.pdf

Dill, J. C. (1981). An application of color graphics to the display of surface curvature. In *Proceedings of the 8th annual conference on Computer graphics and interactive techniques* (pp. 153-161). ACM Publishing. https://doi.org/10.1145/800224.806801

Farin, G. (2014). *Curves and surfaces for computer-aided geometric design: A practical guide*. Elsevier.

Farin, G., Hoschek, J., & Kim, M. S. (Eds.). (2002). *Handbook of computer aided geometric design*. Elsevier. https://doi.org/10.1016/B978-0-444-51104-1.X5000-X

Garcia, D. R., Linke, B. S., & Farouki, R. T. (2021). Optimised routine of machining distortion characterization based on Gaussian surface curvature. In *2nd International Conference of the DFG International Research Training Group 2057–Physical Modeling for Virtual Manufacturing (iPMVM 2020)* (pp. 1-17). Schloss Dagstuhl-Leibniz-Zentrum für Informatik. https://doi.org10.4230/OASIcs.iPMVM.2020.5

Gatzke, T., Grimm, C., Garland, M., & Zelinka, S. (2005). Curvature maps for local shape comparison. In *International Conference on Shape Modeling and Applications 2005 (SMI'05)* (pp. 244-253). IEEE Publishing. https://doi.org/10.1109/SMI.2005.13

Hahmann, S. (1999). Visualisation techniques for surface analysis. In C. Bajaj (Ed.), *Advanced visualization techniques* (pp. 49-74). JohnWiley.

Hu, G., Wu, J., & Qin, X. (2018). A novel extension of the Bézier model and its applications to surface modeling. *Advances in Engineering Software*, *125*, 27-54. https://doi.org/10.1016/j.advengsoft.2018.09.002

Ismail, N. H. M., & Misro, M. Y. (2020). Surface construction using continuous trigonometric Bézier curve. In *AIP Conference Proceedings* (Vol. 2266, No. 1, p. 040012). AIP Publishing LLC. https://doi.org/10.1063/5.0018101

Magid, E., Soldea, O., & Rivlin, E. (2007). A comparison of Gaussian and mean curvature estimation methods on triangular meshes of range image data. *Computer Vision and Image Understanding*, *107*(3), 139-159. https://doi.org/10.1016/j.cviu.2006.09.007

Marsh, D. (2005). *Applied geometry for computer graphics and CAD*. Springer Science & Business Media. https://doi.org/10.1007/b138823

Misro, M. Y., Ramli, A., & Ali, J. M. (2017). Quintic trigonometric Bézier curve with two shape parameters. *Sains Malaysiana*, *46*(5), 825-831. http://dx.doi.org/10.17576/jsm-2017-4605-17

Misro, M. Y., Ramli, A., & Ali, J. M. (2019). Extended analysis of dynamic parameters on cubic trigonometric Bézier transition curves. In *2019 23rd International Conference in Information Visualization–Part II* (pp. 141-146). IEEE Publishing. https://doi.org/10.1109/IV-2.2019.00036

Oxman, N. (2007). Get real towards performance-driven computational geometry. *International Journal of Architectural Computing*, *5*(4), 663-684. https://doi.org/10.1260/147807707783600771

Piegl, L., & Tiller, W. (1996). *The NURBS book*. Springer Science & Business Media. https://doi.org/10.1007/978-3-642-59223-2

Pressley, A. N. (2010). *Elementary differential geometry*. Springer Science & Business Media. https://doi.org/10.1007/978-1-84882-891-9

Razdan, A., & Bae, M. (2005). Curvature estimation scheme for triangle meshes using biquadratic Bézier patches. *Computer-Aided Design*, *37*(14), 1481-1491. https://doi.org/10.1016/j.cad.2005.03.003

Seidenberg, L. R., Jerard, R. B., & Magewick, J. (1992). Surface curvature analysis using color. In *Proceedings Visualization'92* (pp. 260-267). IEEE Publishing. https://doi.org/10.1109/VISUAL.1992.235200

Tan, X., & Zhu, Y. (2019). Quasi-quintic trigonometric Bézier curves with two shape parameters. *Computational and Applied Mathematics, 38*(4), 1-13. https://doi.org/10.1007/s40314-019-0961-y

Zain, S. A. A. A. S. M., Misro, M. Y., & Miura, K. T. (2021). Generalised fractional Bézier curve with shape parameters. *Mathematics*, *9*(17), Article 2141. https://doi.org/10.3390/math9172141

Zheng, J., & Sederberg, T. W. (2003). Gaussian and mean curvatures of rational Bézier patches. *Computer Aided Geometric Design*, *20*(6), 297-301. https://doi.org/10.1016/j.cagd.2003.06.002